chemistry proceedings

MDPI

Proceeding Paper

Design, Synthesis and Studies of Novel Imidazoles †

Priyanka Chandra *, Swastika Ganguly and Manik Ghosh *

Department of Pharmaceutical Sciences and Technology, Birla Institute of Technology, Ranchi 835215, Jharkhand, India; swastikaganguly@bitmesra.ac.in

* Correspondence: priyankachandra78@gmail.com (P.C.); manik@bitmesra.ac.in (M.G.)

† Presented at the 25th International Electronic Conference on Synthetic Organic Chemistry, 15–30 November 2021; Available online: https://ecsoc-25.sciforum.net/.

Abstract: Twenty-five novel imidazole analogs of **26(a–r)** and **27(a–g)** were designed, based on Quantitative Structure Activity Relationship (QSAR)studies. The designed compounds were subjected to molecular docking studies and predictive Absorption, Dissolution, Metabolism, Excretion (ADME) studies were performed. Molecular docking studies were performed in the active site of HIV-1-reverse transcriptase PDB ID: 1RT2 and glucosamine-fructose-6-phosphate animotransferase PDB ID: 2VF5. AutoDock tools v1.5.6 was used for the molecular docking studies. The binding mode analysis of the compounds was carried out. Docking studies suggested that all the compounds showed good interactions, i.e., H-bonding interactions and pi-pi interactions when compared to the standard compounds, i.e., nevirapine (in the case of PDB ID:1RT2) and metronidazole (in the case of PDB ID:2VF5). The predictive ADME studies also showed that all the compounds have drug-like properties. The results show that these compounds can be synthesized and further explored for their possible antimicrobial and antiviral activities.

Keywords: imidazole; QSAR; molecular docking; binding mode analysis; ADME

check for updates

Citation: Chandra, P.; Ganguly, S.; Ghosh, M. Design, Synthesis and Studies of Novel Imidazoles. *Chem. Proc.* **2022**, *8*, 78. https://doi.org/10.3390/ecsoc-25-11628

Academic Editor: Julio A. Seijas

Published: 12 November 2021

Publisher's Note: MDPI stays neutral with regard to jurisdictional claims in published maps and institutional affiliations.

1. Introduction

Compounds containing the imidazole (**1**) nucleus exhibit various activities, viz. antiprotozoal [1–3], antibacterial, antifungal, antiviral, and other various activities [1].

The various drugs that are used in the clinical practice as effective antiprotozoal, antiviral, antibacterial, and antifungal agents containing the imidazole nucleus are azomycin (**2**), metronidazole (**3**), secnidazole (**4**), ornidazole (**5**), benznidazole (**6**), tinidazole (**7**), nimorazole (**8**), megazol (**9**), dimetridazole (**10**), carnidazole (**11**), panidazole (**12**), misonidazole (**13**), clotrimazole (**14**), isoconazole (**15**), miconazole (**16**), butoconazole (**17**), econazole (**18**), oxiconazole (**19**), climbazole (**20**), ketoconazole (**21**), sertaconazole (**22**), flutrimazole (**23**), eberconazole (**24**), and luliconazole (**25**) [1,4–17] (Figure 1).

Human Immunodeficiency Virus is a single-stranded RNA virus that belongs to the retroviridae family. It leads to the development of a deadly disease called AIDS [18]. The enzyme reverse transcriptase helps in the reverse transcription of cDNA, and plays a crucial role in the life cycle of the virus. HIV infections are blocked by targeting various steps of the life cycle of the virus, such as the cell attachment of the virus to human, virus's entry to cell, uncoating of virus, etc. Various enzymes such as reverse transcriptase, protease, and integrase play a vital role in different processes of the viral life cycle and various classes of drugs help in inhibiting these enzymes, such as non-nucleoside reverse transcriptase inhibitors (NNRTIs), nucleoside reverse transcriptase inhibitors (NRTIs), protease inhibitors, nucleotide reverse transcriptase inhibitors (NtRTIs), etc. HIV is subcategorized into two types: HIV-1 and HIV-2, causing infections worldwide and infections confined only to West Africa, respectively. The mechanisms of action of the various classes of drugs are different, thus acting in different phases of HIV infection and subsequently inhibiting the entry and growth of the virus within the host body [19–21]. Imidazole

derivatives have been found to exhibit antibacterial effects as well [1]. The antibacterial effects of 1-alkyl imidazole derivatives increase as the number of carbons in the alkyl chain increases up to nine carbons. Additionally, substitution of methyl and nitro groups at 2- and 4-positions, respectively, on the imidazole ring increases the antibacterial activity of the scaffold [22]. Antibacterial activity can be targeted through various pathways; one is through the inhibition of the hexosamine metabolism pathway [23]. The blocking of this pathway is utilized in this current study for checking the antibacterial effects of the designed compounds.

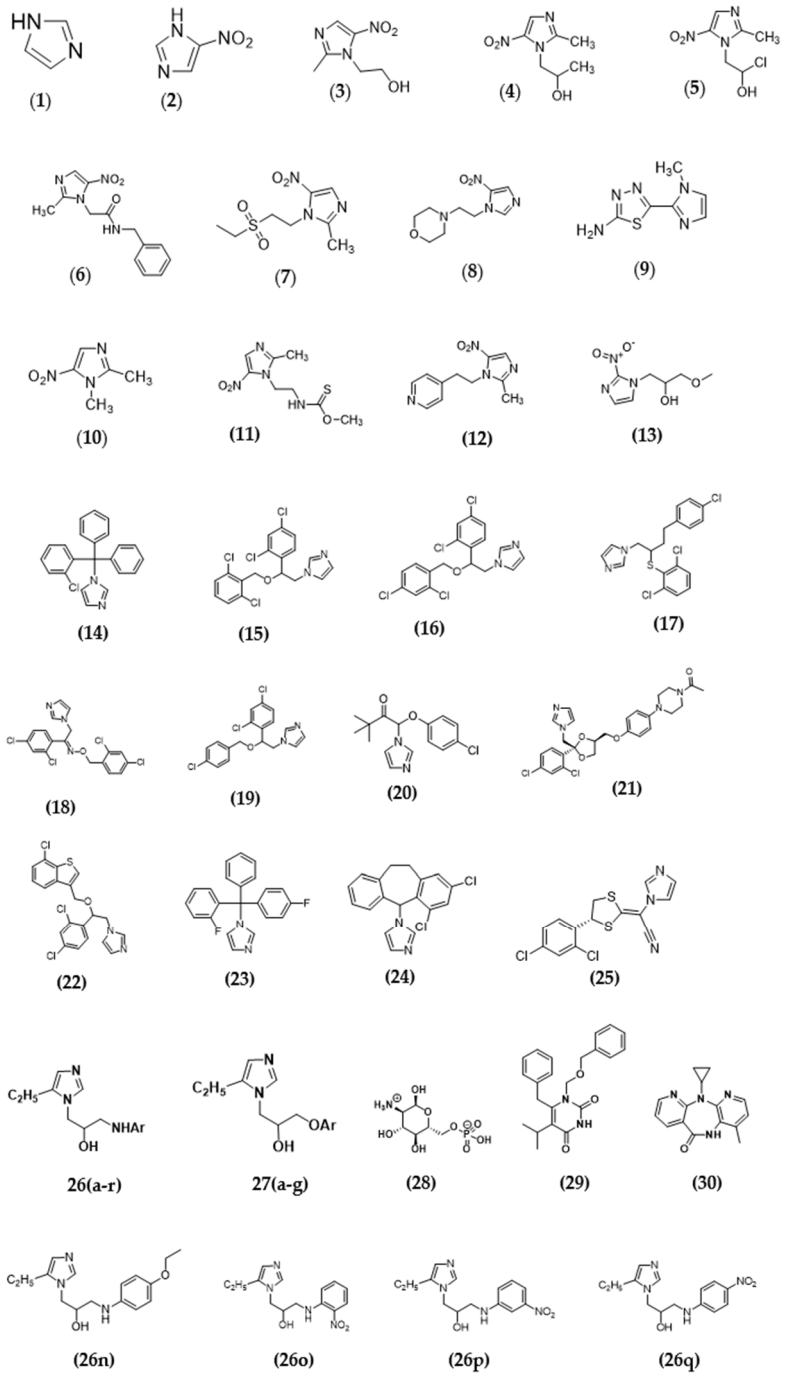

Figure 1. Structures of compounds.

2. Materials and Methods

Autodock v 4.5.6 was used for carrying out the computational studies [24], installed in an HP Precision workstation (Radeon Graphics) with an Intel Core 3 quad processor and 8 GB of RAM, with the operating system as Windows 10.

- **Docking Strategies:**

The binding of drugs in various binding sites can be predicted by using molecular docking studies. For structure-based design of drugs in pharmaceutical sciences, it is a very commonly used method. The different conformations by which it binds to the target site can be easily analyzed by this method. Binding affinity has an important role in rational drug design.

In the present study, we used two receptors, viz. HIV-1-reverse transcriptase, PDB ID: 1RT2 and glucosamine-fructose-6-phosphate animotransferase PDB ID: 2VF5. The internal ligands present in the receptors are TNK (**29**) and GLP (**28**), respectively. The standard drugs that are used for docking the receptors are nevirapine (**30**) and metronidazole (**3**), respectively.

In HIV-1-reverse transcriptase PDB ID: 1RT2, the non-nucleoside inhibitory binding pocket (NNIBP) is formed due to the changes in conformation of the 3D structure of reverse transcriptase, which is induced by the non-competitive binding of NNRTIs. Various amino acid residues that are present in NNIBP play a major role in the interaction with NNRTIs [25].

In glucosamine-fructose-6-phosphate animotransferase PDB ID: 2VF5, the catalytic activation occurs due to glutamine binding after d-fructose 6-phosphate binds to the catalytic site and thereby releases d-glucosamine 6-phosphate as the end product of the first step of hexosamine metabolism [23].

The molecular modelling studies were carried out on two sets of designed novel imidazole analogs, **26(a–r)** and **27(a–g)**, respectively Tables 1 and 2.

- **Molecular Modelling Studies:**
  - **i.** **Protein Preparation:** The X-ray-co-crystallized structures of all of the protein molecules (PDB ID: 1RT2, 2VF5) used in the study were retrieved from the Research Collaboratory for Structural Bioinformatics (RCSB) [26]. From every protein molecule, co-crystallized water molecules were deleted and polar hydrogens were added as well as Gasteiger charges assigned, and it was saved in PDBQT format using AutoDock 4.2.6 software.
  - **ii.** **Ligand Preparation:** All of the ligands were prepared by minimizing their energies using PRODRG server [27]. PDBQT formats of all of the ligands were saved.
  - **iii.** **Receptor grid Generation:** Autogrid was used to generate specific grid maps for each and every ligand. The generation of the grid box was carried out by taking the dimensions of the three coordinates (X, Y, and Z) at 24 × 24 × 24, with grid spacing of 0.100 Å. The values of X, Y, and Z centers were taken according to the crystallographic positions of the native ligand of each receptor.
  - **iv.** **Docking Protocol Validation:** For computational studies, AutoDock 4.2.6 was used. This software was used to predict the different binding mode of co-crystallized ligands as well as test molecules with all of the receptors taken to carry out the study. To carry out the docking procedure, the method was validated to check the robustness of the software. The extracted ligand (previously mentioned) was corrected and then it was redocked using the same protein. The standard drugs were docked into the active site of the respective receptors along with the other test molecules using the same procedure; thereafter, the different conformations were compared. The generated docking scores and conformations of the co-crystallized ligand and the standard drugs were compared with the docking scores of other test molecules to choose the best molecule.

Table 1. List of substituted anilines in **26(a–r)**.

Compound	Ar	Compound	Ar	Compound	Ar
26a	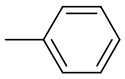	**26g**	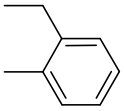	**26m**	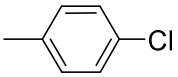
26b	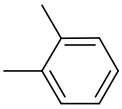	**26h**	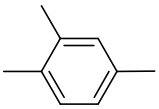	**26n**	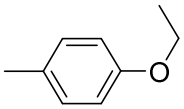
26c	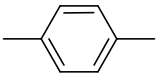	**26i**	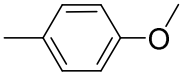	**26o**	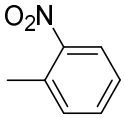
26d	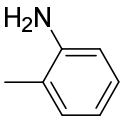	**26j**	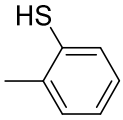	**26p**	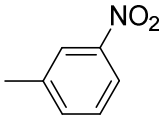
26e	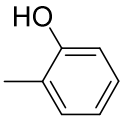	**26k**	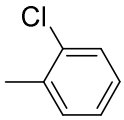	**26q**	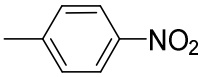
26f	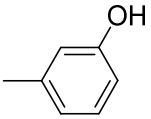	**26l**	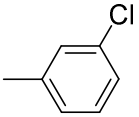	**26r**	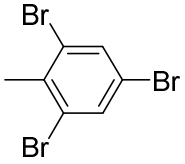

Table 2. List of substituted phenols in **27(a–g).**

Compound	27a	27b	27c	27d	27e	27f	27g
Ar	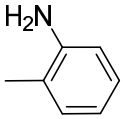	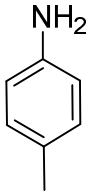	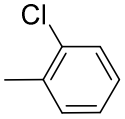	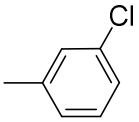	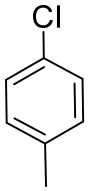	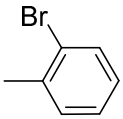	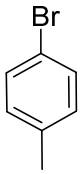

3. Predictive ADME Studies

The predictive ADME studies were carried out by using SwissADME [28], which is a free web tool provided by Swiss Institute of Bioinformatics, using Google chrome web browser installed in a single machine running on a 2.30 GHz Intel Core i5 processor with WINDOWS-8 as the operating system. The analysis of physicochemically important descriptors and pharmacokinetically relevant properties of the ligands can be performed and well predicted by using this online tool. The test compounds were built on the server website (http://www.swissadme.ch (last accessed on 17 May 2021) by using the molecule sketcher (based on Chem Axon's Marvin JS—http://www.chemaxon.com, accessed on 17 May 2021) available on the webpage [28]. This structure was converted to SMILES list (the actual input for the program to run) and then we clicked on Run in order to run the calculations which get activated when the list is not empty. The physicochemical properties

of lipophilicity, drug likeliness, etc., were observed, which was essential to ensure drug-like pharmacokinetic profile while using rational drug design.

4. Results and Discussion

In this work, we considered the crystal structures of HIV-1-reverse transcriptase (PDB Id-1RT2) and the crystal structure of glucosamine-fructose-6-phosphate aminotransferase (PDB Id-2VF5), co-crystallized with the ligands TNK (**29**) and GLP (**28**), respectively. Docking studies were performed using AutoDock Tools (V-4.5.6) on the selected crystal structures. The designed compounds were studied in the non-nucleoside-inhibitory binding pocket of the HIV-1 reverse transcriptase receptor. The docking scores and the binding poses of the different NNRTIs were studied; the results are given in Table 3.

Table 3. Docking scores of the designed compounds in active site of HIV-1-reverse transcriptase PDB ID: 1RT2 and glucosamine-fructose-6-phosphate aminotransferase PDB ID: 2VF5.

Compound	Docking Scores on	
	1RT2	**2VF5**
Native Ligand	−11.9	−7.9
Standard Drug	−9.5	−7.5
26a	−8.3	−6.3
26b	−8.6	−6.2
26c	−8.3	−6.4
26d	−7.9	−6.8
26e	−7.9	−6.8
26f	−7.9	−6.6
26g	−8.6	−6.6
26h	−8.4	−6.4
26i	−7.8	−6.1
26j	−7.9	−6.1
26k	−8.3	−6.3
26l	−8.6	−6.7
26m	−7.9	−6.7
26n	−7.9	−6.7
26o	−8.1	−7.4
26p	−8.2	−7.1
26q	−8.3	−7.4
26r	−5.2	−6.6
27a	−8.3	−7.2
27b	−8.2	−7.2
27c	−8.7	−7.0
27d	−8.7	−7.4
27e	−8.1	−7.1
27f	−8.3	−7.0
27g	−8.0	−7.0

The software used for docking purposes was validated at first to check its reliability for further docking procedures. The internal ligands were removed from the receptors and were redocked into the active site of the protein. Root mean square deviation (RMSD) values of 0.0 Å were obtained for the internal ligands, TNK (**29**) and GLP (**28**), for the HIV-1 reverse transcriptase and glucosamine-fructose-6-phosphate aminotransferase with PDB Id-1RT2 and 2VF5, respectively. As the RMSD values were within the standard limits (i.e., 0.2 Å), the software was used for further docking procedures. In the receptor (PDB Id-2VF5), the docking score of the internal ligand was found to be −7.9; in the same active site, the docking score of the standard drug metronidazole was found to be −7.5. Amongst the designed compounds, the best interaction was shown by two compounds, **26n** and **26o**, with a dock score of −6.7 and −7.4, respectively, in the binding pocket of 2VF5. The binding mode analysis revealed that the compound **26n** had six hydrogen

bond interactions with six amino acids of the binding pocket—ALA602, GLN348, GLU488, VAL399, SER303, and SER401—with a bond length of 2.1 Å, 2.2 Å, 2.4 Å, 2.5 Å, 2.6 Å, and 2.9 Å, i.e., **26n** $_{\text{O-phenyl ring}}$—$_{\text{NH}}$ ALA602 = 2.1 Å, **26n** $_{\text{N-Imidazole ring}}$—$_{\text{NH}}$ GLN348 = 2.2 Å, **26n** $_{\text{NH-phenyl ring}}$—$_{\text{O}}$ GLU488 = 2.4 Å, **26n** $_{\text{OH-propyl chain}}$—$_{\text{O}}$ VAL399 = 2.5 Å, **26n** $_{\text{N-Imidazole ring}}$—$_{\text{OH}}$ SER303 = 2.6 Å, and **26n** $_{\text{OH-propyl chain}}$—$_{\text{O}}$ SER401 = 2.9 Å, whereas the compound **26o** had eight hydrogen-bonding interactions with three amino acids of the binding pocket—SER303, THR 302, and SER401—with a bond length of 2.1, 2.2, 1.9, 2.0, 2.9, 3.1, 3.3, and 3.3 Å, i.e., **26o** $_{\text{O-NO2}}$—$_{\text{NH}}$ SER303 = 2.1 Å, 26o $_{\text{O-NO2}}$—$_{\text{NH}}$ THR302 = 2.2 Å, **26o** $_{\text{NH}}$—$_{\text{O}}$SER401 = 1.9 Å, 26o $_{\text{NH}}$—$_{\text{O}}$SER401 = 2.0 Å, **26o** $_{\text{NH}}$—$_{\text{OH}}$SER401 = 2.9 Å, **26o** $_{\text{OH}}$—$_{\text{O}}$SER401 = 3.1 Å, **26o** $_{\text{OH}}$—$_{\text{NH}}$SER401 = 3.3 Å, and **26o** $_{\text{NH}}$—$_{\text{O}}$SER401 = 3.3 Å (Figures 2 and 3). In the receptor (PDB Id-1RT2), the docking score of the internal ligand was found to be −11.9; in the same active site, the docking score of the standard drug- nevirapine was found to be −9.5. Amongst the designed compounds, the best interaction was shown by two compounds, **26p** and **26q**, with a dock score of −8.2 and −8.3, respectively, in the binding pocket of 1RT2. The binding mode analysis revealed that the compound **26p** had four hydrogen bond interactions with three amino acids of the binding pocket—LYS101, LYS103, and VAL106—with a bond length of 2.3 Å, 2.3 Å, 2.6 Å, and 2.2 Å, i.e., **26p** $_{\text{OH-propyl chain}}$—$_{\text{O}}$ LYS101 = 2.3 Å, **26p** $_{\text{NH-phenyl ring}}$—$_{\text{O}}$ LYS103 = 2.3 Å, **26p** $_{\text{OH-propyl chain}}$—$_{\text{NH}}$ LYS103 = 2.6 Å, and **26p** $_{\text{NO-phenyl ring}}$—$_{\text{NH}}$ VAL106 = 2.2 Å; similarly, the compound **26q** had three hydrogen bond interactions with three amino acids of the binding pocket—VAL106, LYS103, and TYR316—with a bond length of 2.0 Å, 2.7 Å, and 2.8 Å, i.e., **26q** $_{\text{NO-Benzene}}$—$_{\text{NH}}$ VAL106 = 2.0 Å, **26q** $_{\text{OH-phenyl ring}}$—$_{\text{NH}}$ LYS103 = 2.7 Å, and **26q** $_{\text{NH- phenyl ring}}$—$_{\text{OH}}$ TYR316 = 2.8 Å (Figures 2–5).

(**a**) (**b**)

Figure 2. (**a**) Redocking of co-crystallized ligand GLP (**28**) in the binding pocket of glucosamine-fructose-6-phosphate synthase (2VF5). Ligand is shown as orange line model and the amino acid residues interacting with the ligands are shown as green line model. Hydrogen bond interactions (2.048, 1.989, 1.881 Å) with amino acid residues of glucosamine-fructose-6-phosphate synthase are shown in green dotted spheres. (**b**) Binding mode of standard drug metronidazole (**3**) in the binding pocket of glucosamine-fructose-6-phosphate synthase (2VF5). Ligand is shown as multicolor ball and stick model and the amino acid residues interacting with the ligands are shown as green line model. Hydrogen bond interactions (2.144, 2.067, 2.178, 2.002, 1.755 Å) with amino acid residues of glucosamine-fructose-6-phosphate synthase are shown in green dotted spheres.

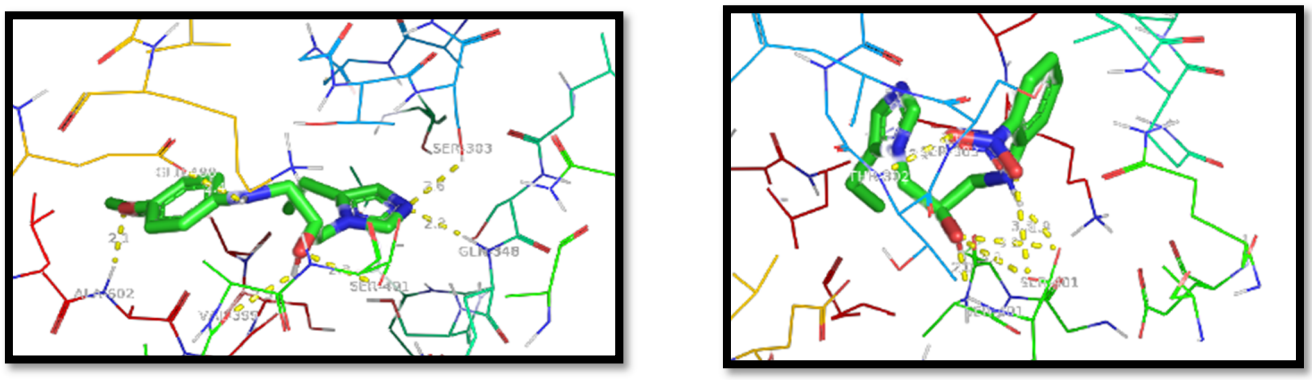

(**a**) (**b**)

Figure 3. (**a**) Docking of compound **26n** in the binding pocket of glucosamine-fructose-6-phosphate synthase (2VF5). Ligand is shown as green line model and the amino acid residues interacting with the ligands are shown as conventional colored line model. Six hydrogen bond interactions (2.4, 2.5, 2.6, 2.2, 2.1, 2.9 Å) with amino acid residues of glucosamine-fructose-6-phosphate synthase are shown in yellow dotted lines. (**b**) Docking of compound **26o** in the binding pocket of glucosamine-fructose-6-phosphate synthase (2VF5). Ligand is shown as green line model and the amino acid residues interacting with the ligands are shown as conventional colored line model. Eight hydrogen bond interactions (2.0, 3.3, 3.1, 1.9, 3.3, 2.2, 2.1, 2.9 Å) with amino acid residues of glucosamine-fructose-6-phosphate synthase are shown in yellow dotted lines.

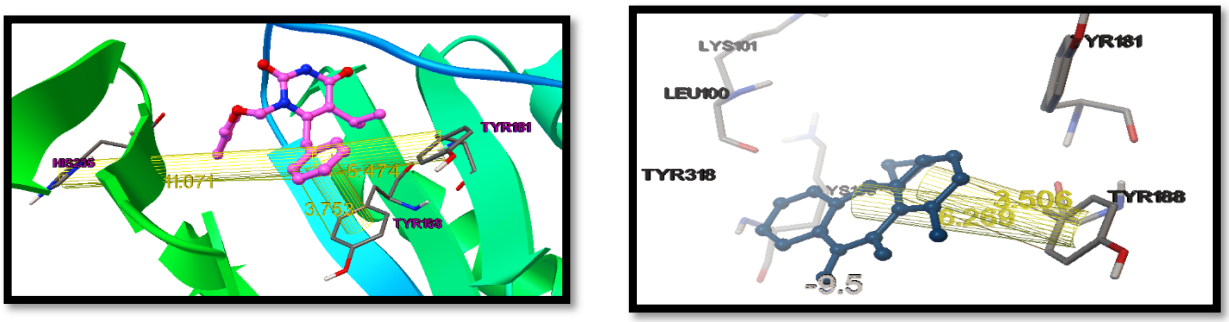

(**a**) (**b**)

Figure 4. (**a**) Redocking of co-crystallized ligand TNK (**29**) in the binding pocket of HIV-1 reverse transcriptase (1RT2). Ligand is shown as pink line model and the amino acid residues interacting with the ligands are shown as conventional colored line model. Π-bond interactions (3.753, 5.474, 11.071 Å) with amino acid residues of HIV-1 reverse transcriptase are shown as lines. (**b**) Binding mode of standard drug nevirapine (**30**) in the binding pocket of HIV-1 reverse transcriptase (1RT2). Ligand is shown as blue-colored ball and stick model and the amino acid residues interacting with the ligands are shown in conventional colored line model. Π-bond interactions (6.269, 3.506 Å) with amino acid residues of HIV-1 reverse transcriptase are shown as lines.

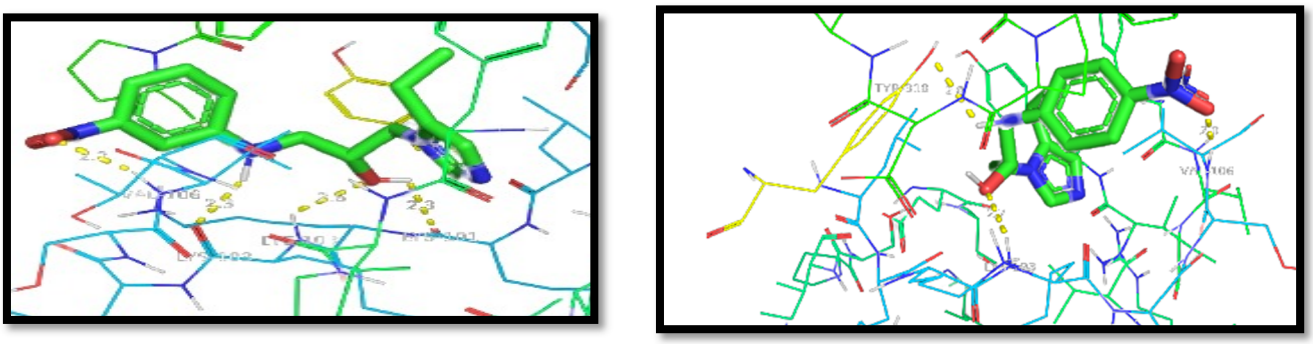

(**a**) (**b**)

Figure 5. (**a**) Docking of compound **26p** in the binding pocket of HIV-1 reverse transcriptase (1RT2). Ligand is shown as green line model and the amino acid residues interacting with the ligands are shown as conventional colored line model. Four hydrogen bond interactions (2.2, 2.3, 2.6, 2.3 Å) with amino acid residues of HIV-1 reverse transcriptase are shown in yellow dotted lines. (**b**) Docking of compound **26q** in the binding pocket of HIV-1 reverse transcriptase (1RT2). Ligand is shown as green line model and the amino acid residues interacting with the ligands are shown as conventional colored line model. Three hydrogen bond interactions (2.0, 2.7, 2.8 Å) with amino acid residues of HIV-1 reverse transcriptase are shown in yellow dotted lines.

Predictive ADME Studies-

The most important descriptors are reported in Table 4, which are required for predicting the drug-like properties of the ligands.

Table 4. Predictive ADME studies of the designed compounds.

Compound	Mol. Wt.	HBA	HBD	MR	TPSA	Log P O/W	Solubility (mg/)mL	Lipinski	Veber's	Leadlikeness
26a	245.32	4	2	72.28	35.5	1.30	1.30	Yes	Yes	No
26b	259.35	4	2	77.63	35.5	1.56	1.55	Yes	Yes	Yes
26c	259.35	4	2	77.63	35.5	1.56	2.01	Yes	Yes	Yes
26d	260.33	5	3	75.02	61.52	0.47	2.24	Yes	Yes	Yes
26e	261.32	5	5	73.48	55.73	0.47	1.52	Yes	Yes	Yes
26f	261.32	5	3	73.48	55.73	0.47	1.52	Yes	Yes	Yes
26g	273.37	4	2	82.44	35.5	1.81	9.23	Yes	Yes	Yes
26h	273.37	4	2	82.99	35.5	1.81	9.17	Yes	Yes	Yes
26i	275.35	5	2	78.21	44.73	0.73	7.09	Yes	Yes	Yes
26j	277.39	4	2	80.24	74.3	1.3	3.15	Yes	Yes	Yes
26k	279.77	4	2	77.11	35.5	1.56	1.99	Yes	Yes	Yes
26l	279.77	4	2	77.11	35.5	1.56	1.99	Yes	Yes	Yes
26m	279.77	4	2	77.11	35.5	1.56	1.99	Yes	Yes	Yes
26n	289.37	5	2	83.01	44.73	0.98	4.15	Yes	Yes	No
26o	290.32	7	2	74.47	38.74	0.15	8.55	Yes	Yes	Yes
26p	290.32	7	2	74.47	38.74	0.15	8.55	Yes	Yes	Yes
26q	290.32	7	2	74.47	38.74	0.15	8.55	Yes	Yes	Yes
26r	482.21	4	2	96	35.5	2.41	3.81	Yes	Yes	No
27a	261.32	3	2	74.46	73.3	0.44	1.59	Yes	Yes	Yes
27b	280.75	3	1	75.06	47.28	1.53	1.93	Yes	Yes	Yes
27c	280.75	3	1	75.06	47.28	1.53	1.93	Yes	Yes	Yes
27d	280.75	3	1	75.06	47.28	1.53	1.93	Yes	Yes	Yes
27e	325.2	3	1	77.75	47.28	1.65	1.09	Yes	Yes	Yes
27f	325.2	3	1	77.75	47.28	1.65	1.09	Yes	Yes	Yes

5. Conclusions

Imidazole analogs (**26a–r**) and (**27a–g**) were designed based on QSAR studies. Docking studies and predictive ADME studies were performed on the designed analogs. Binding mode analysis was carried out in the active site of glucosamine-fructose-6-phosphate synthase (PDB ID: 2VF5) and HIV-1 reverse transcriptase (PDB ID: 1RT2) for all the designed compounds. The binding mode studies suggested that, amongst the designed compounds, maximum compounds showed comparable interactions to the interactions obtained from the standard drug used, and few compounds had shown even better interactions than the standard drug used, in both the receptors. Compounds **26n** and **26o** showed better interactions in the active site of glucosamine-fructose-6-phosphate synthase (PDB ID: 2VF5), and compounds **26p** and **26q** showed better interactions in the active site of HIV-1 reverse transcriptase (PDB ID: 1RT2) than the standard drugs used in both of them, i.e., metronidazole (**5**) and nevirapine (**30**), respectively. The predictive ADME studies suggested that all the compounds were lead-like and can be synthesized for their further exploration.

Author Contributions: Conceptualization, S.G. and M.G.; methodology, S.G.; software, S.G. and M.G.; data curation, S.G.; writing—original draft preparation, P.C.; writing—review and editing, S.G. and P.C.; supervision, S.G. and M.G.; project administration, S.G. and M.G. All authors have read and agreed to the published version of the manuscript.

Funding: No external funding was received in this research.

Institutional Review Board Statement: Not applicable.

Informed Consent Statement: Not applicable.

Data Availability Statement: Not applicable.

Acknowledgments: The authors would like to acknowledge the Department of Pharmaceutical Sciences and Technology, Birla Institute of Technology, Mesra, Ranchi.

Conflicts of Interest: The authors declare no conflict of interest.

References

1. Block, J.H., Jr.; Beale, J.H. *Wilson and Gisvold's Textbook of Organic Medicinal and Pharmaceutical Chemistry*, 11th ed.; Lippincotts Williams and Wilkins: Philadelphia, PA, USA, 2004; p. 504.
2. Butler, K.; Howes, H.L.; Lynch, J.E.; Pirie, D.K. Nitroimidazole Derivatives. Relationship between Structure and Antitrichomonal Activity. *J. Med. Chem.* **1967**, *10*, 891–897. [CrossRef] [PubMed]
3. Tweit, R.C.; Muir, R.D.; Ziecina, S. Nitroimidazoles with Antibacterial Activity against Neisseria Gonorrhoeae. *J. Med. Chem.* **1977**, *20*, 1697–1700. [CrossRef] [PubMed]
4. Mital, A. Synthetic Nitroimidazoles: Biological Activities and Mutagenicity Relationships. *Sci. Pharm.* **2009**, *77*, 497–520. [CrossRef]
5. Edwards, D. Nitroimidazole drugs-action and resistance mechanisms: Mechanism of action. *J. Antimicrob. Chemother.* **1993**, *31*, 9–20. [CrossRef] [PubMed]
6. Raether, W.; Hänel, H.; Ha, H. Nitroheterocyclic Drugs with Broad Spectrum Activity. *Parasitol. Res.* **2003**, *90* (Suppl. 1), S19–S39. [CrossRef] [PubMed]
7. Hall, B.S.; Wilkinson, S.R. Activation of benznidazole by trypanosomal type I nitroreductases results in glyoxal formation. *Antimicrob. Agents Chemother.* **2012**, *56*, 115–123. [CrossRef] [PubMed]
8. Finar, I.L. Stereochemistry and chemistry of natural products. *Org. Chem.* **2002**, *2*, 622–629.
9. Veraldi, S. Isoconazole nitrate: A unique broad-spectrum antimicrobial azole effective in the treatment of dermatomycoses, both as monotherapy and in combination with corticosteroids. *Mycoses* **2013**, *56*, 3–15. [CrossRef] [PubMed]
10. Fischer, J.; Ganellin, C.R. *Analogue-Based Drug Discovery*; John Wiley & Sons: New York, NY, USA, 2006; p. 509. ISBN 9783527607495.
11. Seidman, L.S.; Skokos, C.K. An evaluation of Butoconazole nitrate 2% Site Release® vaginal cream (Gynazole-1®) compared to fluconazole 150 mg tablets (Diflucan®) in the time to relief of symptoms in patients with vulvovaginal candidiasis. *Infect. Dis. Obstet. Gynecol.* **2005**, *13*, 197–206. [CrossRef] [PubMed]
12. Wigger-Alberti, W.; Kluge, K.; Elsner, P. Clinical effectiveness and tolerance of climbazole containing dandruff shampoo in patients with seborrheic scalp eczema. *Praxis* **2001**, *90*, 346–1349.
13. Becker, K.L. *Principle and Practice of Endrocrinology and Metabolism*; Lippincotts Williams and Wilkins; Wiley: Philadelphia, PA, USA, 2001; p. 1197. ISBN 9780781717502.

14. Croxtall, J.D.; Plosker, G.L. Sertaconazole. *Drugs* **2009**, *69*, 339–359. [CrossRef] [PubMed]
15. Alomar, A.; Videla, S.; Delgadillo, J.; Gich, I.; Izquierdo, I.; Forn, J.; Muntañola, A.A.; Masoliver, A.A.; Corominas, A.B.; Montesinos, E.B.; et al. Flutrimazole 1% dermal cream in the treatment of dermatomycoses: A multicentre, double-blind, randomized, comparative clinical trial with bifonazole 1% cream. *Dermatology* **1995**, *190*, 295–300. [CrossRef] [PubMed]
16. Rovati, R.A.; Mestres, R.C. Dichloro-Substituted Imidazole Derivatives as Antifungal Agents. U.S. Patent 07887103, 19 May 1993.
17. Hiroyoshi, K.; Yoshiki, N.; Masanori, Y. Antifungal Agent, Its Compound, Production Thereof and Its Usage. Japan Patent 1997100279A, 15 April 1997.
18. Turner, B.G.; Summers, M.F. Structural biology of HIV. *J. Mol. Biol.* **1999**, *285*, 1–32. [CrossRef] [PubMed]
19. Singh, R.; Gupta, S.; Singh, J.; Arsi, T. Azoles as non-nucleoside reverse transcriptase inhibitors (NNRTIs): Mini review. *Int. J. Pharm. Sci. Res.* **2017**, *8*, 29.
20. De Clercq, E. New approaches toward anti-HIV chemotherapy. *J. Med. Chem.* **2005**, *48*, 1297–1313. [CrossRef] [PubMed]
21. De Clercq, E. The design of drugs for HIV and HCV. *Nat. Rev. Drug Discov.* **2007**, *6*, 1001–1018. [CrossRef]
22. Miller, M.W.; Howes, H.L.; Kasubick, R.V.; English, A.R. Alkylation of 2-methyl-5- nitroimidazole. Some potent antiprotozoal agents. *J. Med. Chem.* **1970**, *13*, 849–852. [CrossRef] [PubMed]
23. Mouilleron, S.; Badet-Denisot, M.A.; Golinelli-Pimpaneau, B. Ordering of C-terminal loop and glutaminase domains of glucosamine-6-phosphate synthase promotes sugar ring opening and formation of the ammonia channel. *J. Mol. Biol.* **2008**, *377*, 1174–1185. [CrossRef] [PubMed]
24. Lindstrom, W.; Morris, G.M.; Weber, C.; Huey, R. *AutoDock 4. The Scripps Research Institute*; Molecular Graphics Laboratory: La Jolla, CA, USA, 2008.
25. Hopkins, A.L.; Ren, J.; Esnouf, R.M.; Willcox, B.E.; Jones, E.Y.; Ross, C.; Miyasaka, T.; Walker, R.T.; Tanaka, H.; Stammers, D.K.; et al. Complexes of HIV-1 reverse transcriptase with inhibitors of the HEPT series reveal conformational changes relevant to the design of potent non-nucleoside inhibitors. *J. Med. Chem.* **1996**, *39*, 1589–1600. [CrossRef] [PubMed]
26. RCSB PDB. Available online: http://www.rcsb.org/pdb (accessed on 10 February 2021).
27. Prodrg 2 Server. Available online: http://prodrg1.dyndns.org/ (accessed on 15 April 2021).
28. SwissADME. Available online: http://www.swissadme.ch (accessed on 17 May 2021).